

520-32

1284 N93 - 19433.1

P-11

SETI Low-Frequency Feed Design Study for DSS 24

P. H. Stanton and P. R. Lee

Ground Antennas and Facilities Engineering Section

The Search for Extraterrestrial Intelligence Sky Survey project requires operation from 1 to 10 GHz on the beam waveguide (BWG) antenna DSS 24. The BWG reflectors are undersized in the 1- to 3.02-GHz range, resulting in poor performance. Horn designs and a method for implementing 1- to 3.02-GHz operation on DSS 24 are presented. A combination of a horn and a shaped feed reflector placed above the main reflector is suggested. The horn and feed reflector could be hidden in the RF shadow of the subreflector and struts. Results from computer analysis of this design indicate that adequate performance could be achieved.

I. Introduction

The DSS 24 34-m beam waveguide (BWG) antenna will be used for the Search for Extraterrestrial Intelligence (SETI) Sky Survey project over a frequency range of 1 to 10 GHz. The antenna's BWG reflectors are undersized for low noise operation at the low end of this frequency range. Therefore, an alternate method of feeding the antenna from 1 to 3.02 GHz is presented in this article. A corrugated, 29-dB-gain horn located at the Cassegrainian focus would give acceptable RF performance but would be physically large and would block the normal BWG transmission path. To reduce the size of the feed horn and facilitate swift clearing of the BWG path for normal DSN operation, a smaller feed horn in combination with a movable shaped reflector could be used instead. This feed reflector would sit over the BWG aperture in DSS 24's main reflector during SETI operations (see Fig. 1(a)) and would be moved into a storage position during DSN operations.

The SETI horn-reflector combination could be hidden in the RF shadow of the subreflector and struts as shown in Fig. 1(b). Major RF system requirements¹ are listed in Table 1.

II. Horn Design and Analysis

Two small-aperture, corrugated horns were used to cover the lower frequency range of the SETI sky survey (horns number one and number two would operate over the ranges of 1 to 1.73 GHz and 1.61 to 3.02 GHz, respectively). The aperture diameter of each of these horns was constrained to three wavelengths, at their lowest operating frequency, in order to help limit its weight and cost. The

¹ G. A. Zimmerman, *Search for Extra-Terrestrial Intelligence Microwave Observing Project Sky Survey Element*, 1720-4100 (internal document), Jet Propulsion Laboratory, Pasadena, California, November 12, 1991.

output flare angles of the horns were adjusted along with the shape of the feed reflector to empirically arrive at an acceptable performance across the two frequency ranges.

Once the frequency range, aperture size, and output flare angle were established, the detailed wideband horn design followed the procedures outlined in [1]. The corrugation profile of the 1- to 1.73-GHz horn is shown in Fig. 2, with its various sections labeled in accordance with [1] (mode converter, frequency transition, angle transition, and output flare).

The corrugated feedhorns were analyzed with a JPL computer program² that uses modal field-matching techniques to determine the transverse electric (TE_{mn}) and transverse magnetic (TM_{mn}) scattering matrix of the horns [2]. From the scattering matrix, the return loss and aperture fields were known. Using the radiation integral, the radiation patterns of the horns were calculated from the aperture fields. Table 2 summarizes the performance of the horns at several frequencies.

III. Feed Reflector Design and Analysis

The shaped feed reflector was designed to optimize system performance at the lowest frequencies, where system spillover was expected to be the highest and to result in higher noise temperature and lower gain. The center of the feed reflector was chosen so that the feed reflector would be located a little above the main reflector. To approximate the location of the first geometric optics (GO) focal point of the feed reflector, a 25-dB horn pattern was used to illuminate the subreflector. This pattern was moved along the axis of the subreflector, and the overall gain of the system was calculated using JPL computer programs³ that employ physical optics (PO) techniques. At the location resulting in the best gain, the far-field phase center of the horn pattern was 437 cm above F1, the focal point of the main reflector and subreflector system [see Fig. 1(a)]. The first GO focal point of the feed reflector was placed 445 cm from the reflector. The second GO focal point was placed in the desired location of the feedhorn far-field phase center. This location was chosen so that the horns would be close to the feed reflector without blocking reflected radiation. The resulting shape was an ellipsoid.

² D. J. Hoppe, *Scattering Matrix Program for Ring-Loaded Circular Waveguide Junctions* (internal document), Jet Propulsion Laboratory, Pasadena, California, August 3, 1987.

³ R. E. Hodges and W. A. Imbriale, *Computer Program POMESH for Diffraction Analysis of Reflector Antennas* (internal document), Jet Propulsion Laboratory, Pasadena, California, February 1992.

The reflector parameters, horn location, and horn flare angle were varied until the performance was acceptable in the 1- to 1.73-GHz range. The performance was then evaluated in the 1.61- to 3.02-GHz range. The horn location and flare angle were varied to achieve acceptable performance. Other reflector parameters were also tried, but the performance was not improved. Figure 3 shows the final reflector design.

The main reflector and subreflector system was designed to work optimally with a 29-dB pattern that has its near-field phase center at F1 and using an observation distance to the subreflector. How the system performs with the GO focal point of the feed reflector so far above F1 was investigated. The phase centers (PC's) of the 1-GHz and 3.02-GHz patterns generated from the horn and feed reflector combination were calculated in the far field and at various distances (R equals observation radius) in the near field (see Fig. 4). As the observation distance moved further into the near field, the phase center moved along the z -axis in a negative direction. Defocus curves of antenna system gain versus feed reflector location were generated by moving the patterns along the axis of the antenna system (see Fig. 5). At the high-frequency limit, the far-field phase center of a focused system is located at the focal point of the ellipsoidal reflector, which is 508 cm above the reflector.

At 1 GHz, the far-field phase center is 208 cm above the feed reflector. The reflector is only about 10 wavelengths in diameter at 1 GHz, so the system will not focus well in any case, but it appears to be somewhat in focus. With the feed reflector at the design location and using an observation distance to the subreflector, the near-field phase center is 7 cm below F1. Using the best gain location from Fig. 5(a), which yields only a 0.05-dB increase in gain, the near-field phase center is 69 cm below F1. Since a wavelength is 30 cm long, the phase centers are reasonably close to F1. At this long wavelength, the system is fairly insensitive to movement of the feed reflector along the main reflector axis.

At 3.02 GHz, the horn and feed reflector system is out of focus, causing the far-field phase center of the reflected pattern to be 155 cm below the reflector. With the feed reflector at the design location, and using an observation distance to the subreflector, the near-field phase center is 320 cm below F1. With a wavelength of 9.9 cm at 3.02 GHz, the phase center is very far from F1. Performance at this frequency could be improved by redesigning the feed reflector to move the near-field phase center close to F1. Simply moving the feed reflector does not improve performance, as shown in the defocus curve of Fig. 5(b).

In an attempt to focus the system some and increase the overall gain, the subreflector was moved along its axis. By moving the subreflector 1.6 cm towards the main reflector, the gain was increased by 0.16 dB.

IV. Results

Table 3 summarizes the antenna system performance as calculated with the PO programs. In the 1- to 1.73-GHz band, the system performs well at one horn location. In the 1.61- to 3.02-GHz band, however, the horn must be moved to four different locations to achieve acceptable performance.

A study of the BWG at 1 GHz was performed using $\cos^n(\Theta)$ patterns as the horn input. The best gain-to-noise temperature ratio (G/T) achieved was 28.24 dB, with a gain of 47.74 dB and a noise temperature of 83.16 K. Compared to the results from horn number one plus the shaped reflector, the noise temperature increases 56.69 K, the gain decreases 2.02 dB, and the G/T decreases 7.30 dB.

V. Conclusion

DSS 24, operating in its normal configuration with the BWG, performs unacceptably at the low frequencies in the SETI 1- to 10-GHz range. By putting a horn and shaped reflector above the main reflector, the BWG could be bypassed, and acceptable performance could be achieved. The horn and shaped reflector would have minimal impact on the other DSS 24 operations since the horn and reflector would be placed in the RF shadow of the subreflector and struts.

The results presented in this article indicate that the suggested configuration would meet SETI system requirements with the two exceptions of noise temperature and beam efficiency. The noise temperature is slightly high in the lower frequencies of both the 1- to 1.73-GHz band and the 1.61- to 3.02-GHz band; however, the G/T is higher than the target G/T over the entire frequency range. The beam efficiency is lower than the system requirements over most of the 1- to 3.02-GHz range. The minimum beam efficiency is 81 percent at 2.21 GHz, and the system requirement is 90 percent over the entire range.

References

- [1] B. M. Thomas, G. L. James, and K. L. Greene, "Design of Wide-Band Corrugated Conical Horns for Cassegrain Antennas," *IEEE Transactions on Antennas and Propagation*, vol. AP-34, no. 6, pp. 750-757, June 1986.
- [2] G. L. James and B. M. Thomas, "TE₁₁ to HE₁₁ Cylindrical Waveguide Mode Converters Using Ring-Loaded Slots," *IEEE Transactions on Microwave Theory and Techniques*, vol. MTT-30, no. 3, pp. 278-285, March 1982.

Table 1. System requirements.

Parameter	Required value
Noise temperature	≤ 25 K
Polarization	RCP ^a and LCP ^b (simultaneous)
Instantaneous bandwidth	≥ 360 MHz
Aperture efficiency	≥ 65 percent
Beam efficiency	≥ 90 percent

^a Right-circular polarization.
^b Left-circular polarization.

Table 2. Horn performance.

Frequency, GHz	Gain, dB	Return loss, dB (TE ₁₁ mode)	Maximum cross-polarization, dB
1- to 1.73-GHz horn			
1.00	17.0	-33	-33.1
1.15	17.2	-41	-30.6
1.32	18.0	-51	-42.7
1.51	18.6	-49	-37.0
3.02	19.5	-47	-37.3
1.61- to 3.02-GHz horn			
1.61	17.1	-65	-29.8
1.88	18.2	-46	-35.6
2.21	19.0	-50	-47.0
2.58	19.7	-47	-37.8
3.02	20.6	-48	-41.7

Table 3. System performance.

Frequency, GHz	Noise Temperature ^a , K	Gain, dB	G/T, dB/K	Target G/T ^b , dB/K	Aperture efficiency	Beam efficiency
1.0- to 1.73-GHz horn						
1.00	26.47	49.77	35.54	35.18	0.747	0.861
1.15	24.68	50.93	37.01	36.40	0.739	0.871
1.32	22.06	52.08	38.65	37.59	0.731	0.915
1.51	21.10	53.11	39.87	38.76	0.708	0.935
1.73	20.55	54.19	41.06	39.94	0.691	0.945
1.61- to 3.02-GHz horn						
1.61	26.52	53.60	39.37	39.32	0.698	0.814
1.88	24.68	54.92	40.99	40.66	0.692	0.854
2.21	24.02	56.47	42.66	40.07	0.716	0.809
2.58	23.46	57.81	44.10	43.41	0.715	0.830
3.02	23.03	59.10	45.47	44.78	0.703	0.867

^a The noise temperature includes contributions from the sky and atmosphere, the reflectors, the horn, and the low-noise amplifier (LNA) assembly. Sky and atmosphere and LNA assembly values from: JPL-ARC Front-End Design Team, *NASA SETI Common Radio Frequency System Design Team Report* (NASA internal report), Appendix D, p. 6, NASA, Washington, DC, August 1, 1991.

^b The target G/T is for 65-percent aperture efficiency and 25-K noise temperature.

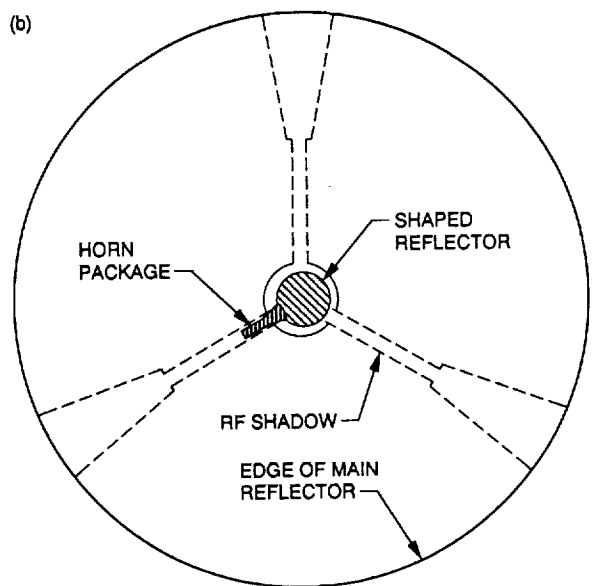
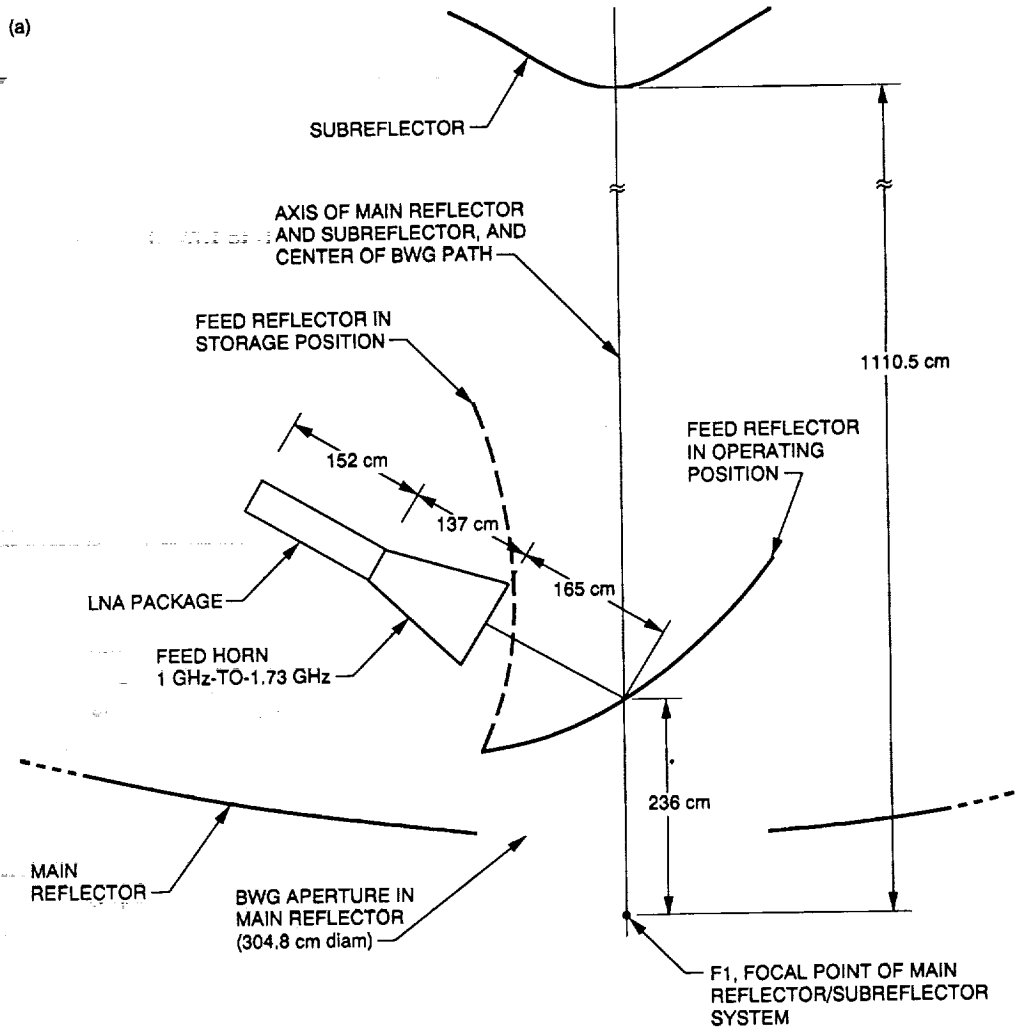


Fig. 1. SETI low-frequency feed system on DSS 24: (a) profile and (b) RF-shadowed region.

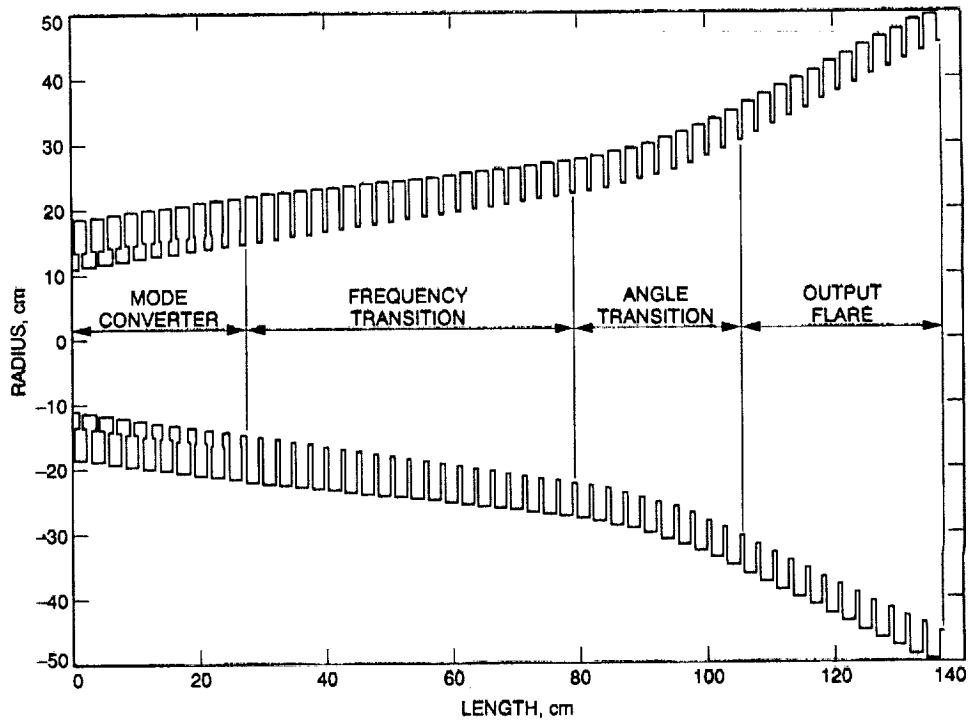


Fig. 2. Profile of 1- to 1.73-GHz horn.

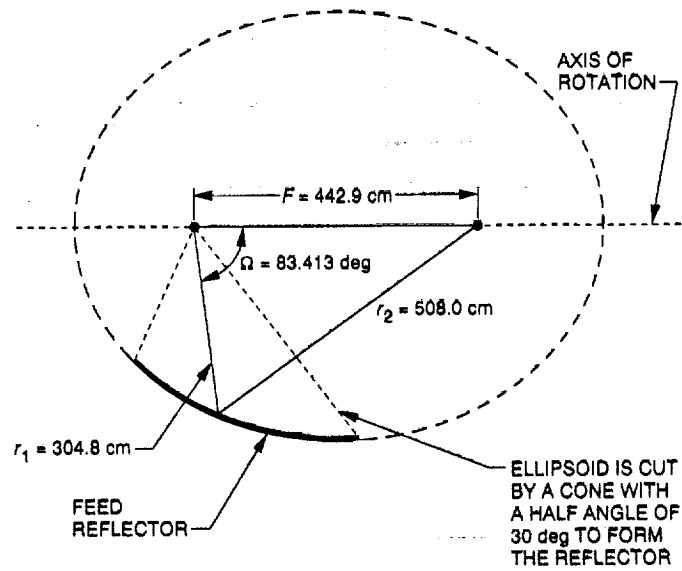


Fig. 3. Feed reflector.

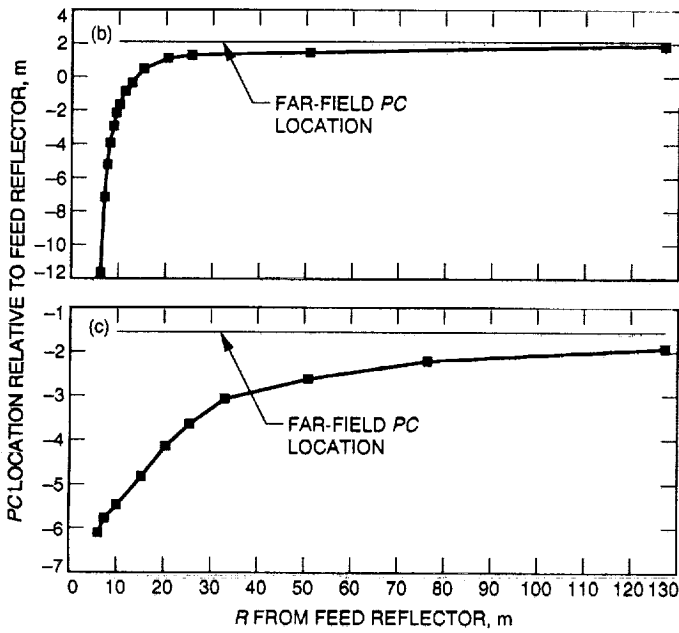
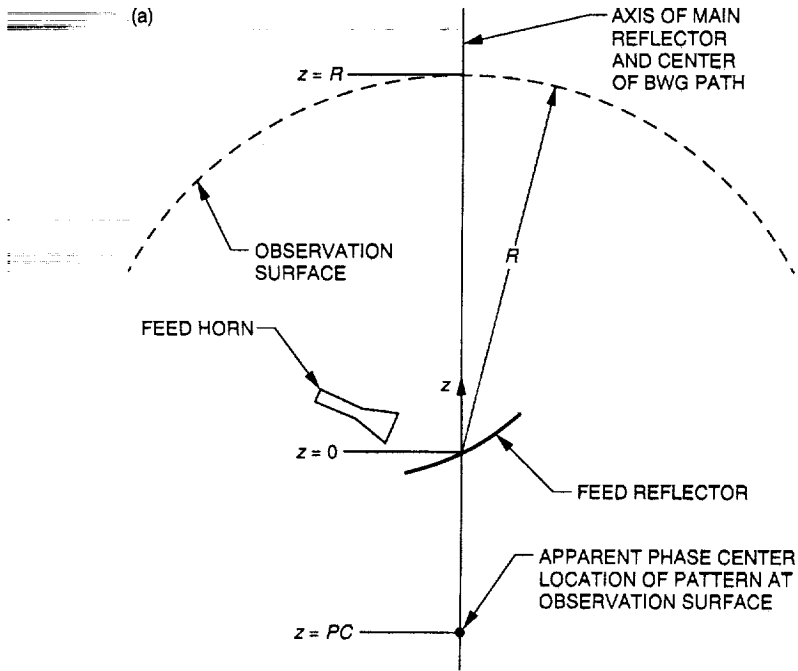


Fig. 4. Phase center location: (a) for horn and feed reflector pattern; (b) versus observation radius at 1 GHz; and (c) versus observation radius at 3.02 GHz.

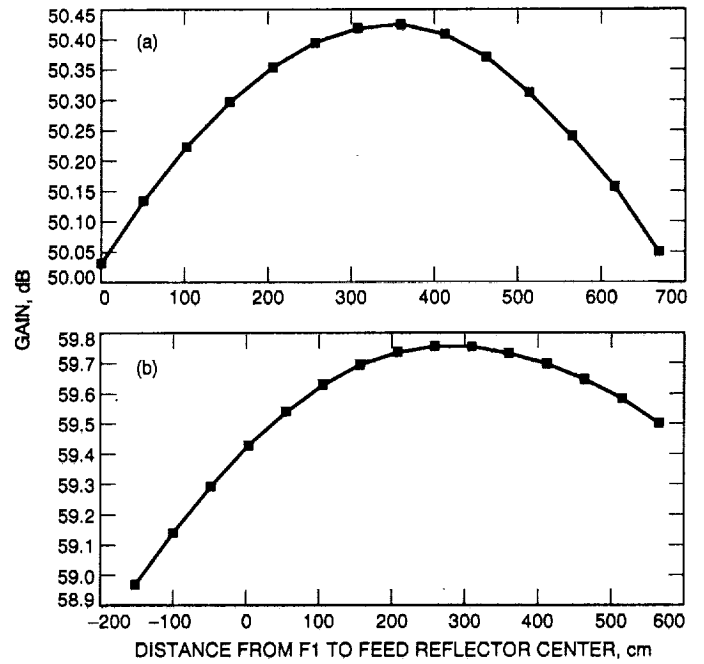


Fig. 5. Gain versus feed reflector location at: (a) 1 GHz and (b) 3.02 GHz.